Effective Collision Cross Sections of the Alkali Atoms in Various Gases

SEYMOUR ROSIN AND I. I. RABI, *Columbia University*

(Received June 12, 1935)

The mean free paths and effective collision cross sections of neutral atoms of Li, Na, K, Rb and Cs were measured in H_2, D_2, He, Ne and A by the method of molecular beams. The beams were sufficiently narrow and the scattering gas was confined to a region sufficiently small that a resolution of one minute of arc was attained. The results show a larger collision cross section in D_2 than in H_2 for all the alkalis with the exception of Li. This effect is interpreted as a consequence of the smaller spacing of the D_2 rotational levels. The results in general are in qualitative agreement with the quantum theory of collisions.

INTRODUCTION

IN the experiments to be described, a beam of atoms was allowed to traverse a limited region containing a gas at various pressures, and the reduction of the intensity of the beam was measured. This reduction is the fraction of the atomic beam scattered out beyond a certain limiting angle, equal here to about one minute of arc. From measurements of this kind an effective mean free path and collision cross section may be calculated, as is shown below. Although the most satisfactory form of this type of experiment would be to scatter a beam of atoms homogeneous in velocity from another such beam, this is out of the question in the present state of technical development. However, experiments which measure the total scattering down to very small angles can yield important information concerning the nature of molecular collisions, since it is in this region that the predictions of various theories are most likely to differ. Such experiments have already been carried out by Mais,[1] who scattered potassium from hydrogen, helium, neon, argon, nitrogen and carbon dioxide. In the experiments described below, the method has been improved by confining the scattering gas to a small region. This has the effect of making the limiting angle smaller and more definite, and enables the utilization of higher pressures, which may be more accurately measured. Beams of lithium, sodium, potassium, rubidium and caesium were each scattered from hydrogen, deuterium, helium, neon and argon.

APPARATUS

The design of the oven (1) (Fig. 1) and the treatment of the alkali before introduction have been described by Rabi and Cohen.[2] The collimating slit which, like the oven slit, is 0.01 mm wide is situated in a holder (2) which may be removed to clean and set the slit jaws, and which is capable of slight adjustment for purposes of alignment in the large partition (3) separating the detecting chamber from the oven chamber. The defining slit holder and the slit jaws are shown in Fig. 2. The first of the stops limiting the height of the beam to 0.25 mm is placed on the oven side of the collimating slit holder. The slit jaws are fitted snugly against the back of the scattering chamber (4) so that the collimating slit itself offers high resistance to gas flow from the scattering chamber into the oven chamber, where scattering is highly undesirable. Since scattering in the collimating slit is also to be avoided, the canal is made only 0.05 mm long.

The scattering chamber is a demountable unit, fastened to the detecting side of the large partition. The back of it is a very thin sheet of

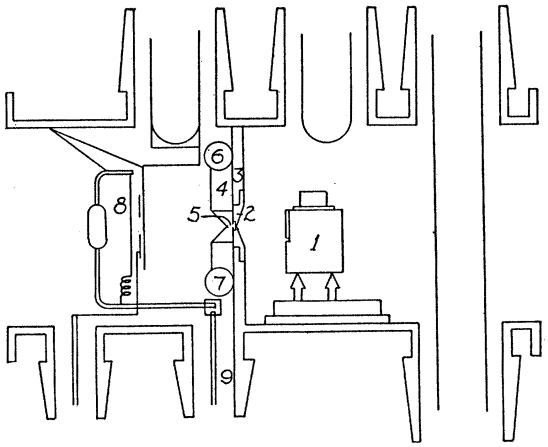

FIG. 1. Apparatus.

[1] Mais, Phys. Rev. **45**, 773 (1934).

[2] Rabi and Cohen, Phys. Rev. **46**, 707 (1934).

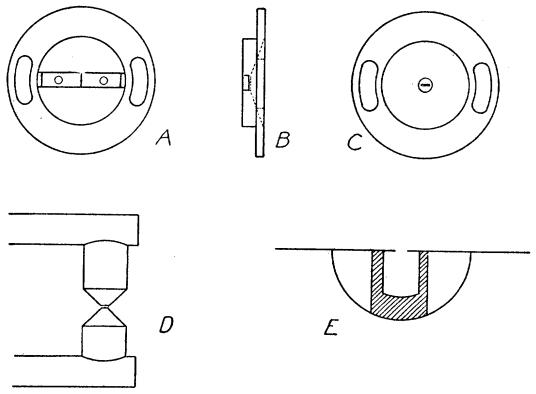

FIG. 2. *A*, Collimating slit jaws and holder, viewed from scattering chamber; *B*, holder, viewed edgewise; *C*, holder, viewed from oven chamber; *D*, scattering chamber, viewed from detecting chamber; *E*, scattering region, horizontal view. Channel is shaded.

metal pierced only by a hole 0.5 mm in diameter to let through the newly defined beam. The form of the chamber is evident from Figs. 1 and 2, consisting of two brass semicylinders soldered to the thin backing sheet and narrowed down at the region of scattering (5). The scattering chamber is connected to the exterior of the apparatus by means of two tubes, one of which, (6) serves to introduce the scattering gas, and the other (7) to lead to a calibrated McLeod gauge, which, since no net flow exists, measures the pressure at the scattering region. A trap serves to prevent mercury atoms from the McLeod from reaching the scattering chamber. The scattering gas is stored in a five liter bulb and admitted to the tube (6) through a constant leak formed by plugging the bore of a stopcock with plaster of Paris. Condensable impurities are frozen out by a Dewar placed between the leak and the scattering chamber and a one-liter bulb is inserted into the path of the gas for stability. During the course of an experiment, a dynamical equilibrium is maintained between the pressure in the five-liter bulb and that in the scattering chamber, and the pressure in the latter may be controlled to any desired value by varying the pressure in the former. The pressure measurements are reproducible to within about two percent over long periods of time. The beam enters the detecting chamber through a channel designed to offer high resistance to gas flow. A horizontal view of the scattering region (5), including the channel is shown in Fig. 2. The open space is 2 mm long, and the length of the channel is one mm and its height 0.25 mm, serving as a beam stop.

The beam is detected by means of a Langmuir-Taylor surface ionization detector[3] and an FP 54 vacuum tube electrometer[4] of sensitivity 10^{-14} amp./mm. The detector in the form of a 0.02 mm tungsten filament (8) (oxide coated when Na and Li are employed), subtends an angle of 1.7 minutes of arc at the scattering chamber. The filament may be rotated about the axis (9) of a ground joint; its position is indicated by a stage micrometer, mounted on the end of an arm 20 cm long attached to the ground joint. The stage, which is calibrated in 0.01 mm markings, is viewed through a fixed microscope. The detecting chamber is exhausted by means of an oil diffusion pump[5] of speed 40 liters/sec., in series with which is a smaller diffusion pump, and a mechanical pump. A 5-liter bulb is placed between the detecting chamber and the pumps for pumping stability.

We now consider the question of where an atom of the beam may undergo a collision. The possible regions are as follows:

(1) In the oven chamber, before the beam is defined. When the oven is hot, residual pressures ranging up to 10^{-5} mm, depending on the temperature of the oven, are measured. The effect is to broaden the beam slightly, and to reduce the intensity of the unscattered beam in the scattering chamber. Since this pressure comes to equilibrium before measurements are taken, the results are unaffected by it. It is also possible that when gas is present in the scattering chamber, enough may leak through the collimating slits to affect the beam in the oven chamber (the inverse beam of Knauer[6]). It was found in test experiments, however, that the pressure in the oven chamber is but 0.02 percent of that in the scattering chamber, and so may be neglected.

(2) In the scattering region proper.

(3) In the channel between the scattering chamber and the detecting chamber. A pressure gradient[7] exists in this region. The average

[3] Taylor, Zeits f. Physik **57**, 242 (1929).
[4] Dubridge and Brown, Rev. Sci. Inst. **4**, 532 (1933).
[5] Zabel, Rev. Sci. Inst. **6**, 54 (1935).
[6] Knauer, Zeits f. Physik **80**, 80 (1933).
[7] Clausing, Physica **9**, 1929.

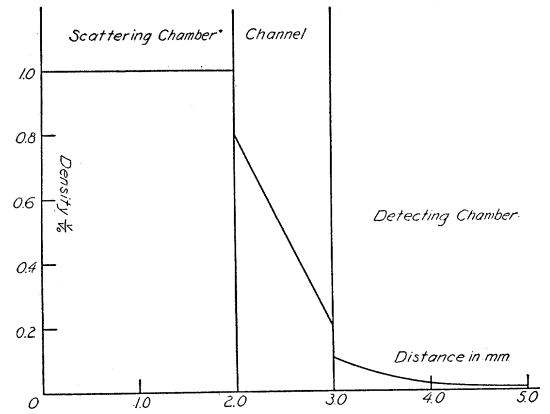

FIG. 3. Relative distribution of density in scattering chamber, channel and cloud.

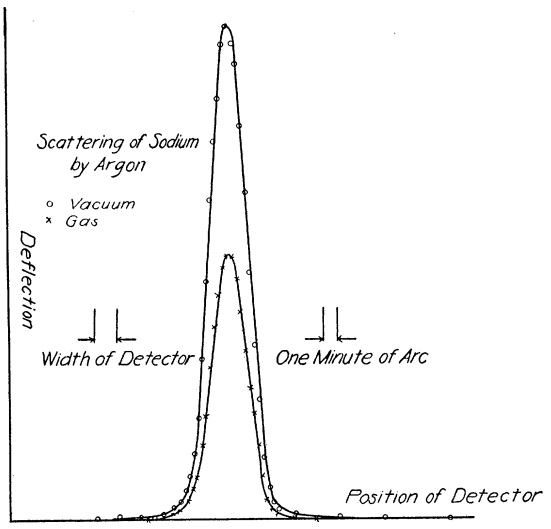

FIG. 4.

pressure is half that in the scattering chamber proper, varying linearly from 0.8 of the scattering chamber pressure to 0.2 of that quantity.

(4) In the detecting chamber where scattering may be ascribed to three sources. A cloud exists close to the scattering chamber, formed by escaping gas molecules. The density of gas escaping from a rectangular opening $2a \times 2b$ is given by

$$\rho = (8/\pi^2) N_0 (a/d) \tan^{-1} (b/d), \qquad (1)$$

where d represents the distance from the radiating rectangle, and N_0 the density on the other side of the opening. The formula is valid for d large compared to a. At the rectangle itself $\rho = N_0/2$, so that the desired function may be plotted. Secondly, residual gas from the walls may serve to reduce the beam. However, if the scattering chamber is evacuated, the McLeod reads flat, which indicates a pressure of 10^{-6} or lower; therefore no appreciable effect arises from this source. Finally, a pressure exists in the detecting chamber due to molecules escaping from the scattering chamber. In test experiments various gas pressures were established in the scattering chamber and the resulting pressure maintained by the pumps in the detecting chamber was always found to be 0.5 percent of that in the scattering chamber.

The density distribution in the scattering region, the channel and the cloud is shown in Fig. 3.

To make our measurements, the scattering chamber was evacuated and the so-called "vacuum beam" investigated by sweeping the detecting filament through the beam and noting the galvanometer deflections at the various settings. This operation was repeated after a suitable amount of some gas was introduced into the scattering chamber. Fig. 4 is a typical result, after proper corrections. The corrections consisted of subtracting the residual positive ion current from the filament, measured by cutting off the beam with a shutter, and also the background due to alkali atoms reflected from the walls of the chamber. Both of these were quite small.

CALCULATIONS AND RESULTS

A large number of curves were secured, involving the different alkalis scattered by each of the gases employed. Upon examination, it is found that the ratio of any ordinate on the gas curve to the corresponding ordinate on the vacuum curve is constant. Thus the gas curve has a form quite similar to that of the vacuum curve, and indeed is indistinguishable from a vacuum curve of lower intensity. The number of molecules scattered close to the beam must be but a small fraction of the total amount scattered, for no scattered atoms are found in this region, within the limits of detection. This result made it unnecessary to take the complete curve each time; in the later stages of the experiment only

the peak values of the gas and vacuum curves, and the pressure in the scattering chamber were measured.

To calculate the mean free paths of the atoms of the beam in the scattering gas, we write

$$P_1=e^{-s_1/\lambda_1}, \quad P_2=e^{-s_2/\lambda_2}\cdots, \tag{2}$$

where P_1, P_2, $\cdots$, etc. are the probabilities that the beam atom will pass through the regions s_1, s_2, $\cdots$, etc. without collision, and λ_1, λ_2, $\cdots$, etc. are the mean free paths. Since the mean free path is assumed to be inversely proportional to the pressure, we write

$$p\lambda=p_0\lambda_0, \tag{3}$$

where p_0 and λ_0 are constants, and p is the pressure. The probability that the atom will pass through all the regions s_1, $s_2\cdots$ etc. without collision is the product of the separate probabilities. We thus have

$$P=e^{-(1/p_0\lambda_0)\int p(s)ds}. \tag{4}$$

The scattering in the various regions is conveniently indicated in Table I. Eq. (4) may be put in a form more suitable for calculation.

$$p_0\lambda_0=0.275p/\log P^{-1}. \tag{5}$$

The mean free path λ_0 at any desired pressure p_0 may now be evaluated. P is the ratio of gas to vacuum intensities.

To test the assumption made in Eq. (3), P^{-1} was varied from 1.3 to 10, and over this large range, $p_0\lambda_0$ was constant within the experimental error. It is to be noted that where the higher pressures were employed no effect was apparent on the results in spite of the fact that the average beam atom made several collisions. Thus it is seen that once a beam atom experiences a collision, the chance it may have of striking the detector through one or more additional collisions is remote.

TABLE I. *Scattering in the various regions. (p is the pressure in the scattering chamber.)*

REGION	s (CM)	AVERAGE PRESSURE	$\int pds$	% OF TOTAL
scattering chamber	0.2	p	$0.2p$	73
channel	0.1	$p/2$	$0.05p$	18
cloud			$0.005p$	2
detecting chamber	4.0	$0.005p$	$0.02p$	7
		Total	$-0.275p$	

The results of this experiment may be expressed by giving the mean free path at some standard pressure. However, since unimportant factors such as the ratio of the masses and temperatures enter into this quantity, it is better to express the results in terms of an effective collision cross section $\pi\sigma_{AG}^2$. The number of collisions made per second by a beam atom with molecules of the scattering gas may be written[8]

$$\Theta=(\pi^{\frac{1}{2}}\nu_G\sigma_{AG}^2/h_Gm_Gc_A)\psi(c_A(h_Gm_G)^{\frac{1}{2}}),$$
$$h_G=1/2kT_G, \tag{6}$$

where the subscripts A refer to the beam atom, and the subscripts G to the scattering gas. ν is the number of molecules per cc, σ_{AG} the effective collision radius, k Boltzmann's constant, T the absolute temperature, m the molecular mass, c the molecular velocity and

$$\psi(x)=xe^{-x^2}+(2x^2+1)\int_0^x e^{-y^2}dy. \tag{7}$$

The mean free path of the atom in question is then c_A/Θ. Now the fraction of atoms striking the filament per second having speeds between c_A and c_A+dc_A is

$$f(c_A)=2(h_Am_A)^2c_A^3e^{-h_Am_Ac_A^2}dc_A. \tag{8}$$

If we average the mean free path over this distribution in the usual way, we secure for the average mean free path of the beam atoms in the scattering gas the following expression

$$\lambda_A=\frac{2}{\pi^{\frac{1}{2}}\nu_A\sigma_{AG}^2}\left(\frac{T_GM_A}{T_AM_G}\right)^2 \times\int_0^\infty \frac{x^5e^{-(T_GM_A/T_AM_G)x^2}dx}{\psi(x)} \tag{9}$$

and for the collision radius

$$\sigma_{AG}^2=\frac{3.30\times10^{-17}}{p_0\lambda_0}\alpha^2\int_0^\infty\varphi(x,\alpha)dx, \tag{10}$$

where $p_0\lambda_0$ is secured from the experimental measurements by means of Eq. (5), $\alpha=T_GM_A/T_AM_G$, and $\varphi(x,\alpha)$ is the integrand in Eq. (9). The

[8] Jeans, *Dynamical Theory of Gases*, third edition, p. 254.

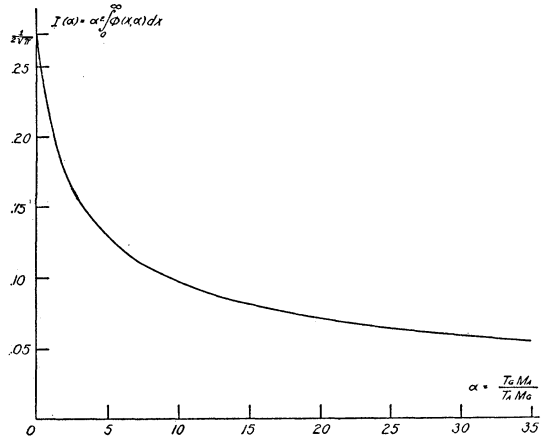

FIG. 5.

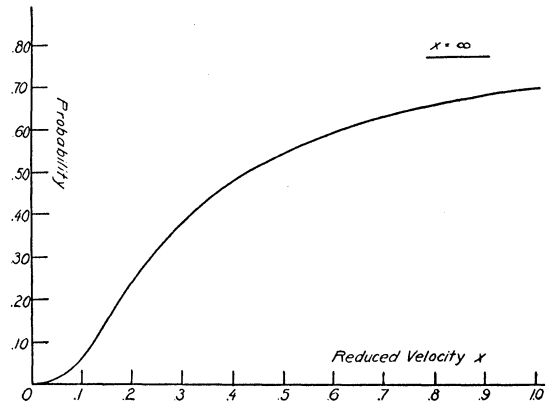

FIG. 6.

integral must be evaluated numerically; it is convenient to express it as a function of α (Eq. 10) and after evaluation at various points to plot it (Fig. 5). Inasmuch as the numerical calculations are somewhat laborious, the points are given in Table II
where

$$I(\alpha)=\alpha^2\int\varphi(x,\alpha)dx.$$

The computation of the σ_{AG}'s as outlined above is not strictly accurate. We computed the average mean free path from Eq. (9) and related this quantity to the experimental value P, the average probability that a beam atom will undergo no collision, by Eq. (5). While the latter relation is accurate for atoms of one velocity it is only an approximation for average values. A more valid procedure would be to average the probabilities.

The mean free path of a beam atom moving with velocity c_A is

$$\lambda_x=x^2/\pi^{\frac{1}{2}}\nu_G\sigma_{AG}{}^2\psi(x), \tag{11}$$

where

$$x=c_A(h_Gm_G)^{\frac{1}{2}}. \tag{12}$$

We average the probability

$$P_x=e^{-s/\lambda_x} \tag{13}$$

over the distribution

$$f(x)=2\alpha^2x^3e^{-\alpha x^2}dx,$$

which is identical with (8).

The average probability is, then,

$$P=2\alpha^2\int_0^\infty \exp\left[-\{s\pi^{\frac{1}{2}}\nu_G\sigma_{AG}{}^2/x^2\}\{xe^{-x^2}+(2x^2+1)\int_0^x e^{-y^2}dy\}-\alpha x^2\right]x^3dx. \tag{14}$$

Although more accurate, this equation is not as convenient to employ as Eq. (9) since the σ_{AG} occurs under the integral sign. Calculation shows, however, that the final results from the two methods are not appreciably different. If the σ_{AG} as found by (9) for a particular case be inserted into (13), a curve such as is shown in Fig. 6 is secured, where the probability that a beam atom will pass through the scattering gas without collision is plotted against its reduced velocity x. The upper curve in Fig. 7 is the distribution $x^3e^{-\alpha x^2}$ where the number of particles is plotted against the reduced velocity. The lower curve is the result of multiplying each of the ordinates in the upper curve by the corresponding ordinate in

TABLE II. *Values of $I(\alpha)$ for a number of values of α.*

α	$I(\alpha)$	α	$I(\alpha)$	α	$I(\alpha)$	α	$I(\alpha)$
0	$1/2\sqrt{\pi}$	0.545	0.236	3.0	0.155	10	0.094
0.05	0.275	0.8	0.221	4.0	0.140	15	0.0813
0.1	0.265	0.9	0.216	5.28	0.127	21	0.0714
0.2	0.256	1.0	0.211	7.0	0.113	25	0.0643
0.3	0.248	2.0	0.173	8.0	0.107	30	0.0589
						35	0.0548

TABLE III. *Product of mean free path and pressure, $p_0\lambda_0$ calculated from Eq. (5) (p_0 is in mm of mercury and λ_0 in cm).*

GAS	Li 860°K	Na 700°K	K 620°K	Rb 590°K	Cs 560°K
H_2	16.2×10^{-4}	8.30×10^{-4}	5.44×10^{-4}	4.24×10^{-4}	3.20×10^{-4}
D_2	18.6	8.74	5.85	4.65	3.65
He	22.6	12.52	8.32	6.50	4.89
Ne	22.5	10.94	7.77	6.65	5.41
A	11.4	5.90	4.22	3.75	3.34

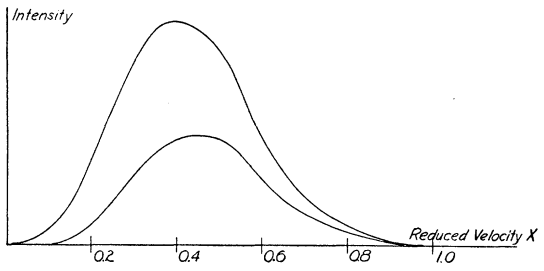

FIG. 7. Distribution of velocities in vacuum and gas beams.

Fig. 6. The upper curve gives the distribution of velocities in the vacuum beam, and the lower that in the scattered beam. Thus we see that after being scattered, the form of the original Maxwellian distribution is lost to some extent, containing a smaller proportion of low velocity atoms, and having the maximum of the distribution shifted somewhat towards the region of higher velocities. The results of previous experiments of this type may be open to the criticism that multiple scattering may have taken place, especially in the low velocity group. Owing to the low angular resolution employed by previous experimenters, the effect of multiple collisions is to give an apparent mean free path which is too large, and an effective collision radius too small.

The accuracy in the mean free path determination is estimated to be within four percent, as determined from variations in the experimental measurements. Using an apparatus with entirely different geometry, Mais obtains values of 7.20A, 6.91A, 8.74A and 11.3A* for the collision radius of potassium, respectively, with hydrogen, helium, neon and argon. Each of the first three are about 0.3–0.4A lower than the values appearing below (see Table IV), but this slight disagreement may be expected since improvement in geometry and confinement to smaller scattering angles would each tend to make the measured mean free path somewhat smaller, and collision radius larger. The precision in the σ_{AG} would be about two percent since the collision radius is proportional to the inverse square root of the mean free path; however, when $\alpha = T_G M_A / T_A M_G$ is large, the determination of σ_{AG} is very sensitive to α, and if the temperatures are not precisely known, some further error will be introduced. This corresponds to the scattering of Rb and Cs in H_2, D_2 and He and the error in σ_{AG} may be four percent. This factor is not so important in the remaining cases.

The mean free path-pressure product $p_0\lambda_0$ calculated from Eq. (5), where p_0 is in mm of mercury and λ_0 in cm, is given in Table III. The average temperature of the oven is given with each alkali; the scattering gases were all approximately at 10°C. It may be pointed out that the large increase found in the mean free path as we pass from the heavier to the lighter alkalis is to be ascribed chiefly to the increased velocity of the atoms of the latter. Furthermore, the variation of the mean free path with velocity of the beam atoms is greater in the lighter than in the heavier scattering gases (note especially the values under K, Rb and Cs); this is also predicted from the theory. The values given here for the mean free path should be useful to the molecular beam experimenter in estimating the pressures necessary for his experiment.

If we insert the values from Table III into Eq. (10), we secure the effective collision cross sections $\pi\sigma_{AG}^2$ and radii σ_{AG}. These are given in Table IV.

TABLE IV. *Values of effective collision cross sections and radii for the alkali atoms in various gases.*

Gas	Lithium		Sodium		Potassium		Rubidium		Caesium	
	σ_{AG}	$\pi\sigma^2_{AG}$	σ_{AG}	$\pi\sigma^2_{AG}$	σ_{AG}	$\pi\sigma^2_{AG}$	σ_{AG}	$\pi\sigma^2_{AG}$	σ_{AG}	$\pi\sigma^2_{AG}$
H_2	6.21	122	7.01	154	7.47	175	7.38	171	7.54	179
D_2	6.32	125	7.62	182	8.54	228	8.24	213	8.34	219
He	5.82	106	6.44	130	7.25	165	6.96	152	7.18	162
Ne	6.18	120	8.24	213	9.10	259	9.23	268	9.56	287
A	9.83	303	11.3	401	13.6	580	13.5	572	13.5	572

The collision radii are expressed in Angstroms and the cross sections in square Angstroms.

DISCUSSION

The results of chief physical interest are given in Table IV. Comparison of the collision cross sections for H_2 and D_2 with the various alkalis shows D_2 to have a larger cross section in all cases except in collision with Li. In view of results[9] on the relative viscosity of H_2 and D_2, it

*The authors communicated with Dr. Mais concerning the large discrepancy in argon, and reconsideration of his original data established that this value should be raised to 13.0A.

[9] H. C. Torrey, Bull. Am. Phys. Soc., No. 1 (1935).

may be assumed that the molecular force fields are the same in both. The difference in collision cross section is therefore very likely connected with the excitation of rotational levels in the molecules. In D_2 the rotational levels are closer together, because of the larger mass.

Although the collision cross sections presented in Table IV are really lower limits, the absence of considerable small angle scattering in the region of a few minutes of arc, as shown by the fact that the beam is not appreciably broadened, implies that they are the real values such as would be obtained from an infinitely narrow beam and detector. The agreement with the results obtained by Mais with beams effectively four and a half times as broad confirms this conclusion. It is interesting in this connection to point out that classically with an attractive van der Waals force varying as r^{-5}, there would be approximately 70 percent of the total scattering above one minute of arc between one and ten minutes; and with an r^{-14} law, about 30 percent would be in this region. The absence of such scattering is, of course, in accord with the predictions of quantum theory.

We take this opportunity to thank Professor Urey and Dr. Christ of the Department of Chemistry for supplying the deuterium, Dr. Bleakney of Princeton for determining its purity on the mass spectrograph and Mr. Torrey and other members of the molecular beam laboratory for their able assistance when needed.